Kinetics and Catalysis, Vol. 46, No. 3, 2005, pp. 422–436. Translated from Kinetika i Kataliz, Vol. 46, No. 3, 2005, pp. 450–465.
Original Russian Text Copyright © 2005 by Vorontsov, Kozlov, Smirniotis, Parmon.

DEDICATED TO THE BORESKOV INSTITUTE OF CATALYSIS

TiO_2 Photocatalytic Oxidation: II. Gas-Phase Processes

A. V. Vorontsov*, D. V. Kozlov*, P. G. Smirniotis, and V. N. Parmon***

** Boreskov Institute of Catalysis, Siberian Division, Russian Academy of Sciences, Novosibirsk, 630090 Russia*

*** University of Cincinnati, Cincinnati, OH 45221-0012 USA*

Received April 30, 2004

Abstract—The results of studies on the TiO_2 photocatalytic oxidation of model air pollutants are summarized. The kinetics of photocatalytic oxidation of CO and the vapors of a number of simple organic substances was studied in detail. It was found that, in the course of reaction, all of the test substances underwent complete mineralization. Gaseous substrates were converted with the participation of several types of reaction centers. The photocatalytic oxidation of sulfur- and phosphorus-containing substances resulted in gradual deactivation of the photocatalyst; however, its activity can be restored by washing the photocatalyst with water. It was found that, along with oxidation, the steps of hydrolysis play an important role in the photocatalytic degradation of air pollutants, such as dimethyl methylphosphonate and 2-chloroethyl sulfide.

INTRODUCTION

Fine air cleaning to remove chemical and biological pollutants is one of the most promising directions in the development of heterogeneous photocatalysis. Traditional air cleaning methods for the removal of trace impurities include adsorption by activated carbon, catalytic combustion, and flame combustion.

These methods possess considerable disadvantages. In fact, adsorption by carbon does not destroy pollutants; it only converts them into adsorbed species, which should be further utilized. Moreover, adsorption by carbon is ineffective in the removal of many highly volatile compounds, such as carbon monoxide and formaldehyde. Toxic substances, for example, dioxins, can be formed upon flame combustion or catalytic combustion. Therefore, additional measures for emission control are required. According to economic evaluations, photocatalytic air cleaning, which does not require large-scale heating, can successfully compete with the above two traditional methods. Indeed, the use of photocatalytic methods requires analogous capital outlays; however, operating costs for the removal of a great number of contaminants are much lower [1].

Among the advantages of photocatalytic air cleaning are its high efficiency at room temperature and atmospheric pressure, low selectivity for the nature of contaminants, and ability to deactivate or even mineralize pathogenic microorganisms that are present in air.

In this work, we summarize the results of our recent experimental studies on the kinetics and mechanism of conversion of a number of typical air contaminants. We consider the photocatalytic oxidation of CO and the vapors of acetone, ethanol, organic sulfides, and dimethyl methylphosphonate on TiO_2 powders.

EXPERIMENTAL

The samples used in this study, the experimental procedure, and the analysis of products and reagents, as well as the instrumentation, were described in the preceding paper [5].

The IR spectra were measured with the use of Vector 22 (Bruker) and Shimadzu 8300 FTIR spectrophotometers.

The photocatalysts in reactors were irradiated with filtered or unfiltered light from a 1000-W xenon lamp or with unfiltered light from a 1000-W DRSh mercury lamp.

In the calculation of the quantum yields of photoprocesses, it was assumed that incident UV light ($\lambda <$ 380 nm) was almost completely absorbed by the samples of pure and modified TiO_2. The quantum yields were calculated from the equation $\varphi = n\frac{W_{ox}}{I} \times 100\%$, where W_{ox} is the rate of photocatalytic degradation of the test substance (mol/s), I is the intensity of incident UV light (moles of quanta per second), and n is the number of quanta required for the complete photocatalytic degradation of the test substance.

RESULTS AND DISCUSSION

1. Photocatalytic Oxidation of Carbon Monoxide

The photocatalytic oxidation of CO in air on TiO_2 prepared by the thermal decomposition of titanyl sulfate was performed in a flow-circulation reaction. The dependence of the rate of photocatalytic oxidation of CO on its concentration in the reactor was described by the Langmuir–Hinshelwood equation. The rate of photocatalytic oxidation of CO reached a maximum value

at a CO concentration in the mixture higher than 40000 ppm. In this case, the quantum efficiency of the process was ~12% with consideration for the fact that the oxidation of each CO molecule requires two photons [2]. At a low CO concentration of 500 ppm, the measured quantum efficiency was ~0.6%. Under the conditions used (temperature, 40°C; concentrations of water vapor and CO, 4000 and 500 ppm, respectively), the intensity of light and the concentration of the reaction product (CO_2) did not have a considerable effect on the quantum efficiency. However, under these conditions, an increase in the temperature significantly accelerated the reaction, and the apparent activation energy was equal to 11 kJ/mol. Because the thermal reaction of catalytic CO oxidation does not occur even at the highest temperature of 160°C, the observed increase in the reaction rate with temperature cannot be attributed to the thermal steps of this simple reaction. It is believed that the rate of photocatalytic oxidation increased with temperature because of competition between CO and H_2O for adsorption onto reaction sites on the surface of TiO_2. Based on data on the heats of adsorption of CO and H_2O, we evaluated the expected apparent activation energy of the photocatalytic oxidation of CO as 7 kJ/mol. This value is consistent with the experimental value of 11 kJ/mol. Although pure titanium dioxide exhibits a moderate photocatalytic activity in CO oxidation, this activity can be increased by an order of magnitude by surface modification with platinum [3].

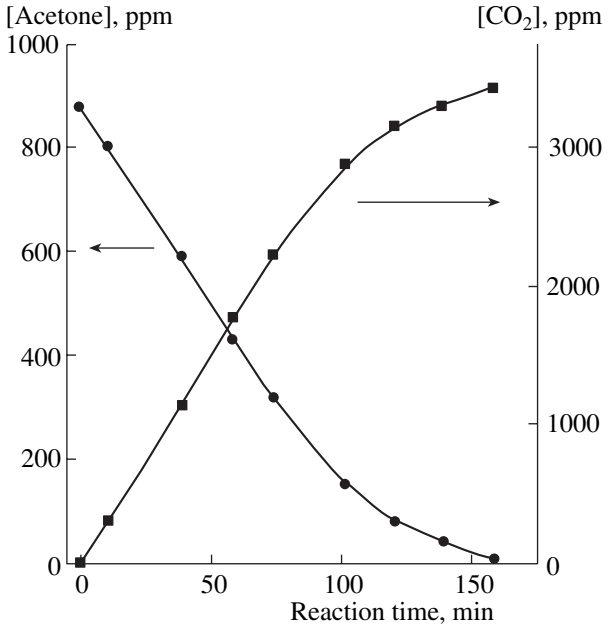

Fig. 1. Photocatalytic oxidation of acetone vapor in air on Hombikat UV 100 TiO_2 in a 449-cm^3 batch reactor. Catalyst weight, 15 mg; illuminated surface area, 3 cm^2; temperature, 25°C; irradiation power, 20 mW/cm^2; water concentration in the gas phase, 5000 ppm (25%). Irradiation was performed with full light from a DRSh-1000 lamp.

2. Photocatalytic Oxidation of Acetone Vapor

Acetone is a material commonly used for studying gas-phase photocatalytic oxidation. This is partly due to the fact that intermediate gaseous substances are not formed in considerable amounts during the oxidation of acetone vapor. As an example, Fig. 1 demonstrates the kinetics of photocatalytic oxidation of acetone vapor on Hombikat UV 100 TiO_2 powder in a small batch reactor. After the introduction of acetone into the reactor, approximately a third of the total amount was adsorbed on the surface of TiO_2 and two-thirds occurred in the gas phase. Because the major portion of acetone occurred in the gas phase, adsorption had almost no effect on the kinetics of its consumption [4, 5]. Therefore, the concentration measured in the gas phase decreased to almost zero in a short time in accordance with the Langmuir–Hinshelwood equation; thus, it is consistent with the mechanism of photocatalytic oxidation with a single type of reaction centers. The concentration of carbon dioxide (the product of the complete oxidation of acetone) linearly increased with reaction time and flattened out at the end of reaction. The absence of other carbon-containing substances from the gas phase is typical of acetone oxidation.

Light is a necessary "reagent" for photocatalytic oxidation. Therefore, an increase in the intensity of a light flux should increase the rate of acetone photooxidation. Figure 2 shows this dependence for the initial reaction rate of complete acetone oxidation. It can be seen that, at low light intensities, the initial rate of the reaction linearly increased with light intensity, whereas it deviated from linearity at high intensities. This type of dependence on light intensity is characteristic of many photocatalytic reactions on semiconductor oxides. In this case, it is likely that the nonlinear portion of the curve is due to an increase in the probability of recombination of photogenerated charge carriers at high light intensities.

The rate of photooxidation can be studied by measuring either the initial rate of reaction in a batch reactor or the steady-state rate in a flow or flow-circulation reactor. We will demonstrate below that these approaches to the measurement of rates do not always give identical results.

Figure 3 demonstrates the dependence of the initial rate of complete oxidation of acetone vapor on the initial concentration of acetone in a batch reactor. The rate curve flattened out at a concentration of about 1000 ppm; it corresponds to the Langmuir–Hinshelwood model with a single type of reaction centers. It is of importance that the adsorption isotherm of acetone retraces the rate curve of photocatalytic oxidation at acetone vapor concentrations lower than 1000 ppm. At higher concentrations, the multilayer adsorption of acetone came into play and the adsorption curve increased, unlike the rate curve of oxidation. Thus, at acetone vapor concentrations lower than 1000 ppm, the rate of

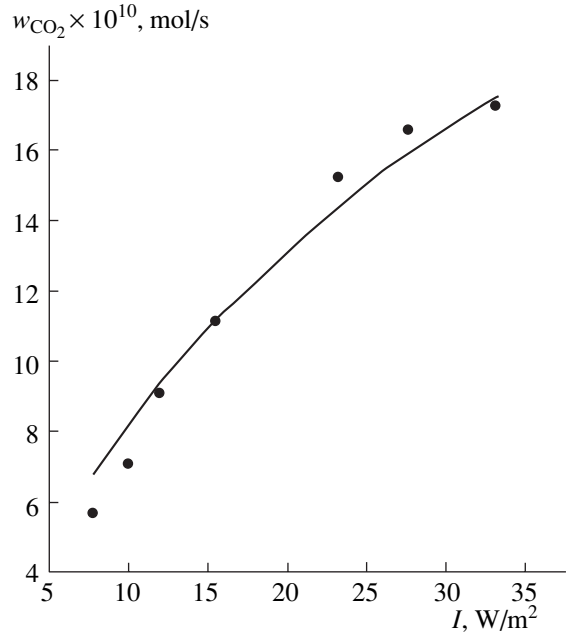

Fig. 2. Dependence of the initial rate of CO_2 buildup (w_{CO_2}) on irradiation intensity (I) in the photocatalytic oxidation of acetone vapor on Hombikat UV 100 TiO_2 under exposure to light with $\lambda = 365$ nm in a batch reactor at 25°C. Initial acetone concentration, 1000 ppm; sample surface area, 3 cm^2.

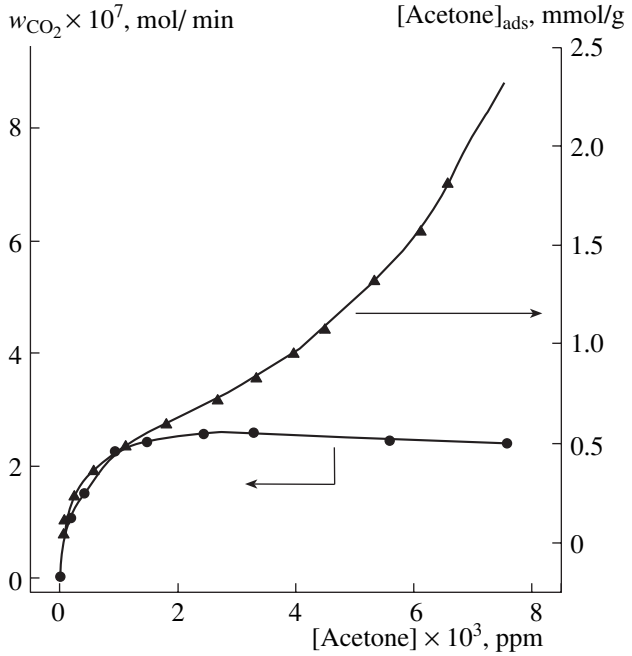

Fig. 3. Dependence of the initial rate of CO_2 buildup (w_{CO_2}) on the initial concentration of acetone in the photocatalytic oxidation of acetone vapor and the isotherm of acetone adsorption on the same sample of Hombikat UV 100 TiO_2. Temperature, 25°C. Irradiation was performed with full light from a DRSh-1000 lamp.

photocatalytic oxidation was directly proportional to the amount of adsorbed acetone. This provides support for the hypothesis that photooxidation occurs in an adsorbed state of molecules on the surface of a photocatalyst. At higher concentrations of acetone vapor, a small decrease in the initial rate of oxidation was observed. It is likely that this decrease was related to a decrease in the accessibility of the surface of TiO_2 to oxygen because of the multilayer adsorption of acetone.

Figure 4 demonstrates the effects of acetone concentration and temperature on the rate of complete photocatalytic oxidation for the reaction performed in a flow-circulation reactor in a steady state [6]. The curves cannot be approximated by the Langmuir–Hinshelwood model with a single type of reaction centers (dashed lines). However, they are adequately described by a model with two types of reaction centers that are characterized by different rate constants of photocatalytic reactions (solid lines in Fig. 4). As the temperature was increased from 40 to 80°C, the rate of photocatalytic oxidation increased by a factor of ~1.5 because of an increase in the reaction rate constant at centers with strong acetone adsorption. As expected, the constants of adsorption on the centers of both types decrease with temperature. Based on IR spectroscopic data, the centers of weak adsorption can be attributed to hydroxyl groups, whereas the centers with strong adsorption can be ascribed to surface titanium atoms.

Thus, two types of reaction centers should be taken into account in the consideration of the test photocatalytic reaction under steady-state conditions. This is essentially different from the model of unsteady-state reaction in a batch reactor; this model implies the consideration of a system with a single type of reaction centers. This difference between the kinetic peculiarities of the process under different conditions can be the consequence of a considerable change in the surface properties of TiO_2 in the steady-state occurrence of the photocatalytic reaction. For example, under steady-state conditions, the accumulation of large amounts of partial oxidation products of the substrate on the surface of the photocatalyst and the partial desorption of water from the surface of TiO_2 are possible. The molecules of acetic acid, which is an intermediate in the complete oxidation of acetone, can also serve as centers for the weak adsorption of acetone through hydrogen bonds.

In the photocatalytic oxidation of acetone vapor under steady-state conditions, it was found that an increase in the temperature above 80–120°C resulted in a decrease in the rate of complete oxidation and in the darkening (i.e., deactivation) of the initial white photocatalyst [3, 6]. The accumulation of partial oxidation products preceded the observed deactivation of the pho-

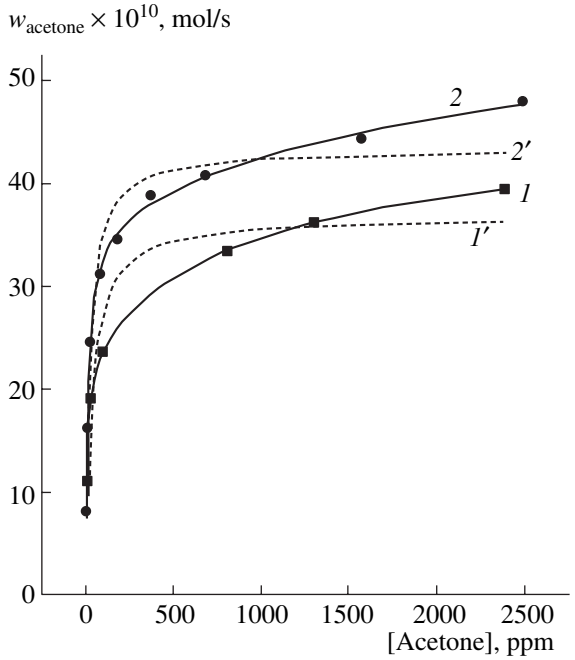

Fig. 4. Dependence of the rate of complete photocatalytic oxidation of acetone vapor ($w_{acetone}$) in air on TiO_2 on acetone concentration at two temperatures: (*1*, *1'*) 40 and (*2*, *2'*) 80°C. Water vapor concentration, 4500 ppm. See the text for comments.

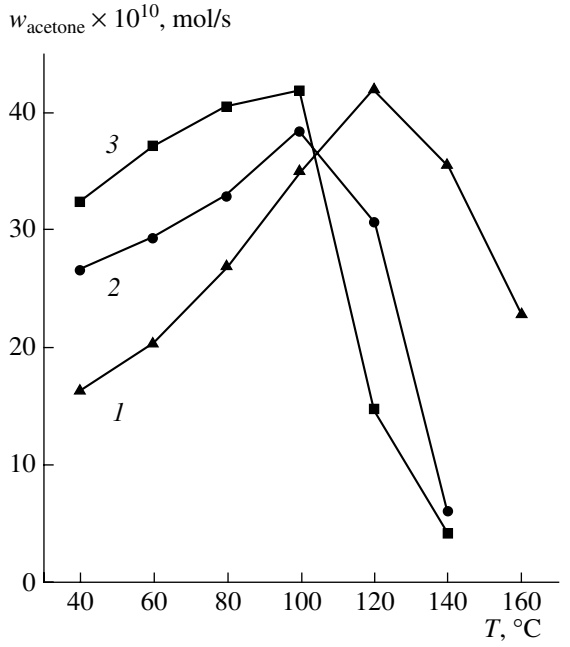

Fig. 5. The temperature dependence of the rate of complete oxidation of acetone vapor ($w_{acetone}$) on TiO_2 under steady-state conditions at three acetone concentrations: (*1*) 50, (*2*) 500, and (*3*) 2000 ppm. Water vapor concentration, 5000 ppm.

tocatalyst, as evidenced by a decrease in the rate of carbon dioxide release and an increase in the rate of acetone consumption at deactivation temperatures. The aldol condensation of acetone with the formation of products that block the access of oxygen molecules to the surface of TiO_2 is the most probable reason for the observed deactivation.

We also studied the effects of air humidity and acetone vapor concentration on the deactivation of TiO_2. Figure 5 shows data on the effect of the acetone vapor concentration. At temperatures lower than 100°C, an increase in the concentration of acetone caused an increase in the rate of deep oxidation. At temperatures higher than 100°C, the character of this dependence changed: the higher the concentration of acetone, the lower the rate. In this case, the maximum rate of complete oxidation shifted to the region of high temperatures with decreasing acetone concentration. This behavior of the rate of photocatalytic oxidation can be associated with the fact that, at a low concentration of acetone, the rate of its condensation on the surface decreased and photocatalyst deactivation slowed down.

As follows from Fig. 6, an increase in the concentration of water vapor had a promoting effect on the deep photocatalytic oxidation of acetone at temperatures higher than 100°C; however, it decreased the rate at temperatures lower than 100°C. The maximum of the rate shifted toward high temperatures with increasing concentration of water vapor. The highest rate of the photocatalytic oxidation of acetone was detected at a water vapor concentration of 15000 ppm and a temperature of 120°C. The positive effect of water observed at deactivation temperatures is also consistent with evidence for a decrease in acetone concentration on the surface of the photocatalyst because of displacement by water. The second reason for the observed effect of water vapor concentration can consist in the inhibition of the aldol condensation of acetone because of water poisoning of active Lewis sites of condensation.

Platinum is an effective catalyst for dark oxidation. Platinum supported on titanium dioxide is favorable for maintaining a high catalyst activity even at the temperatures of rapid catalyst deactivation. Indeed, Fig. 7 shows that the rate of acetone oxidation on platinized titanium dioxide monotonically increased with reaction temperature. In this case, the contribution of acetone oxidation in the absence of light was limited and no higher than 15%. Consequently, platinum participates in the oxidation of acetone reaction intermediates on the surface of titanium dioxide but practically does not participate in the oxidation of parent acetone molecules.

The activity of a platinized photocatalyst at elevated temperatures is many times higher than the activity of pure titanium dioxide [7]. The apparent activation energies of the complete oxidation of acetone on a platinized catalyst under steady-state conditions were 11.5 ± 1.8 kJ/mol for the purely photocatalytic process and 43.7 ± 3.3 kJ/mol for the pure dark reaction.

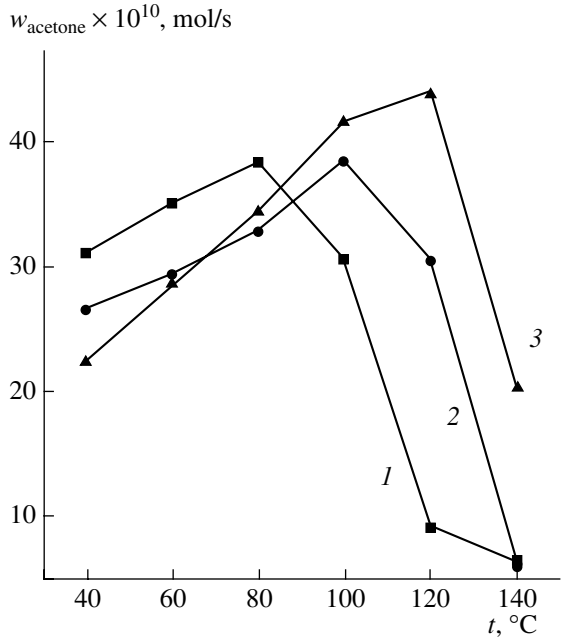

Fig. 6. The temperature dependence of the rate of complete oxidation of acetone vapor ($w_{acetone}$) on TiO_2 under steady-state conditions at three water vapor concentrations: (*1*) 1050, (*2*) 3800, and (*3*) 15000 ppm. Acetone concentration, 500 ppm.

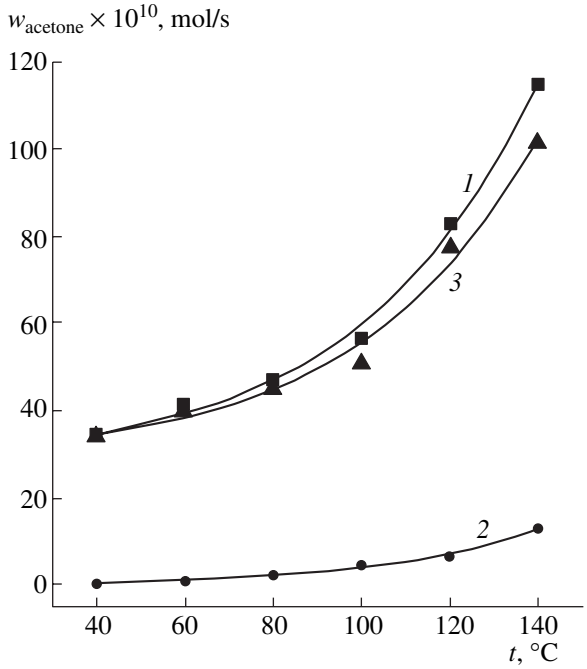

Fig. 7. Rates of deep oxidation of acetone vapor ($w_{acetone}$) on the 0.41% Pt/TiO_2 photocatalyst under steady-state conditions at various temperatures: (*1*) under UV light, (*2*) in the dark, and (*3*) purely photocatalytic reaction. Acetone vapor concentration, 530 ppm; water vapor concentration, 4500 ppm; photocatalyst weight, 38 mg. Illumination was performed with filtered light from a DKSL-1000 xenon lamp (λ = 334 nm).

It is of interest to reveal the factors responsible for an increase in the photocatalytic activity of platinized titania as compared with that of pure titanium dioxide. This is possible when the kinetics of photocatalytic oxidation obeys the Langmuir–Hinshelwood equation. In this case, the effect of platinization on the apparent rate constants of acetone oxidation and adsorption can be found. Figure 8 demonstrates the dependence of the rate of complete acetone oxidation on the concentration of acetone vapor for platinized and pure titanium dioxide. Dashed lines show the approximation of experimental curves by the Langmuir–Hinshelwood equation with a single type of reaction centers. It can be seen that the experimental kinetic curves cannot be described by this approximation. In the approximation of the curves by a model with two types of reaction centers, the agreement with experimental data was much better (solid lines in Fig. 8).

The above data indicate that the rate of photocatalytic oxidation at a low concentration of acetone vapor was higher on platinized titanium dioxide, whereas the rate was higher on pure titanium dioxide at a high concentration of the vapor. Table 1 summarizes the adsorption and kinetic parameters of the deep photocatalytic oxidation of acetone vapor on pure and platinized titanium dioxide for the model with two types of reaction centers. It can be seen that platinization increased the rate constant of oxidation at strong adsorption centers; in this case, the constant of adsorption at these centers also somewhat increased. In contrast, the rate constants of acetone oxidation and adsorption at weak adsorption centers decreased. Because of this, the activity of pure titanium dioxide was higher at high concentrations of acetone. The adsorption constants obtained by measuring the adsorption isotherm of acetone in the dark were dramatically different from the adsorption constants obtained by measuring the rate of the photocatalytic reaction under steady-state conditions. It is believed that this dramatic difference was due to a considerable modification of the surface state of titanium dioxide upon irradiation with UV light or acetone photoadsorption on the surface under the action of UV light. In particular, irradiation resulted in the removal of a portion of adsorbed water molecules and in the liberation of reaction centers, which can become accessible to acetone adsorption.

3. Photocatalytic Oxidation of Ethanol Vapor

The deep photocatalytic oxidation of ethanol vapor is a much more complicated process as compared with the above systems, and a great number of parameters should be taken into account for its quantitative interpretation. As distinct from acetone, a considerable amount of acetaldehyde, a gaseous intermediate of deep oxidation, is formed in the photocatalytic oxida-

tion of ethanol vapor; acetaldehyde competes with ethanol for adsorption sites on the surface of the photocatalyst [3].

Published data on the detection of a number of intermediate products of the photocatalytic oxidation of ethanol both on the surface of TiO_2 and in the gas phase are available. We used *in situ* IR absorption spectroscopy [8] for studying the composition of products in the oxidation of ethanol in a batch reactor (quartz cell). In this cell, by turning a holder with a fixed thin pellet of titanium dioxide, we could either remove or place the pellet of TiO_2 in the optical path of the spectrometer. Thus, we measured either the sum of the spectra of the gas phase and the surface or the spectrum of only the gas phase.

The onset of the photocatalytic oxidation of ethanol was accompanied by the appearance of absorption bands due to acetaldehyde and acetic acid in the IR spectra of the gas phase. The IR spectrum of the surface of titanium dioxide after illumination for 100 min exhibited many absorption bands that corresponded to the adsorbed intermediates of ethanol oxidation (Fig. 9). Table 2 summarizes the assignment of the absorption bands of this spectrum based on published data. The compounds detected on the surface of TiO_2 include acetic acid, acetaldehyde, and carbonates, as well as the carbonyl and carboxyl groups of compounds whose structures were not clearly identified. According to the IR spectroscopic data and published data [9], the reaction path of the photocatalytic oxidation of ethanol on TiO_2 can be described by the following reaction scheme:

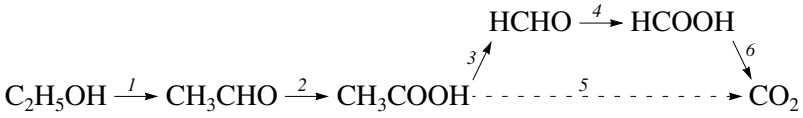

In this reaction scheme, acetic acid can lead to the formation of CO_2 and HCHO as a result of photocatalytic decarboxylation (steps *3* and *5* in the scheme) [10].

The above reaction scheme involves five intermediates, which compete for the same reaction centers and undergo oxidation with different rate constants. Thus, the complete kinetic model of this reaction scheme should include at least ten parameters; because of this, it is problematic to use this model for obtaining reliable kinetic data. However, because only acetaldehyde occurred in considerable amounts in the gas phase during the photocatalytic oxidation of ethanol vapor with a low partial pressure, under these conditions, the following simplified two-step reaction model, which takes into consideration only acetaldehyde as a single gaseous intermediate [11], can be used:

$$CH_3CH_2OH \xrightarrow{1} CH_3CHO \xrightarrow{2} 2CO_2.$$

Figure 10 demonstrates the dependence of the rates of the first and second steps of ethanol oxidation on the concentrations of ethanol and acetaldehyde vapors. The experimental functions cannot be described by the Langmuir–Hinshelwood model with a single type of reaction centers. In accordance with published data [12], adsorption centers that are accessible to only ethanol or only acetaldehyde or to both of the substances simultaneously occur on the surface of TiO_2. Based on this assumption, the rates of the first and second steps of photocatalytic oxidation W_1 and W_2, respectively, should obey the equations

$$W_1 = W_E + \frac{k_E K_E C_E}{1 + K_E C_E + K_A C_A},$$
$$W_2 = \frac{k_A^A K_A^A C_A}{1 + K_A^A C_A} + \frac{k_A K_A C_A}{1 + K_E C_E + K_A C_A}. \quad (1)$$

Table 1. Adsorption and kinetic parameters of the photocatalytic oxidation of acetone vapor in air on unplatinized TiO_2 and platinized titanium dioxide containing 0.41 wt % Pt based on the Langmuir–Hinshelwood model with two types of reaction centers (1 and 2)

Sample	Photocatalytic oxidation of acetone				Adsorption of acetone (in the dark)			
	$k_1 \times 10^{10}$, mol/s	$K_1^{(L)}$, ppm^{-1}	$k_2 \times 10^{10}$, mol/s	$K_2^{(L)}$, ppm^{-1}	$a_1 \times 10^7$, mol/m^2	K_1, ppm^{-1}	$a_2 \times 10^7$, mol/m^2	K_2, ppm^{-1}
TiO_2	24	0.088	23	0.00097	6	0.0026	27	0.00012
Pt/TiO_2	29	0.10	8	0.00035	5	0.0038	29	0.00017

Note: k_1 and k_2 are the rate constants of photocatalytic oxidation of ethanol; $K_1^{(L)}$ and $K_2^{(L)}$ are the constants of ethanol adsorption (under light) on two types of reaction centers under steady-state conditions; a_1 and a_2 are the adsorption values corresponding to monolayer surface coverage; and K_1 and K_2 are the constants of ethanol adsorption on two types of reaction centers in the dark.

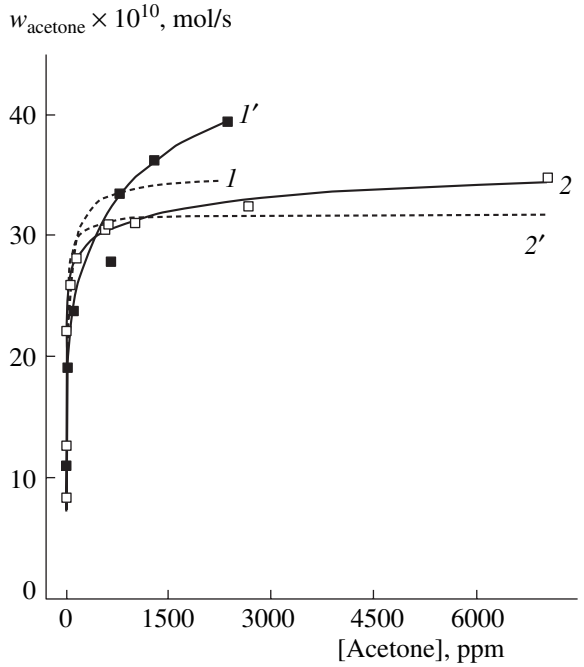

Fig. 8. Dependence of the rate of oxidation of acetone vapor ($w_{acetone}$) under steady-state conditions on acetone concentration: (*1*, *1*') on pure TiO_2 and (*2*, *2*') on 0.41% Pt/TiO_2 with Pt supported by $NaBH_4$ reduction; temperature, 40°C; water vapor concentration, 4500 ppm; photocatalyst weight, 25 mg (in both cases). Illumination was performed with filtered light from a DKSL-1000 xenon lamp (λ = 334 nm). See the text for comments.

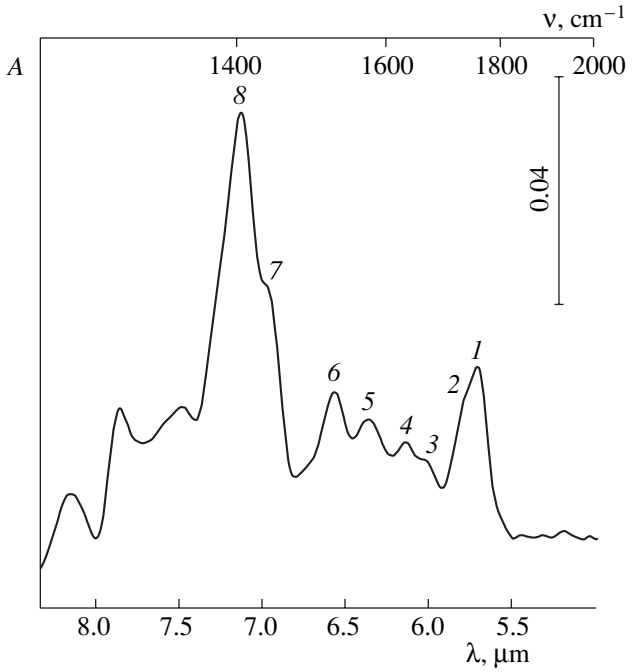

Fig. 9. IR absorption spectrum of TiO_2 after illumination with full light from a DRSh-1000 lamp for 102 min in the presence of ethanol vapor in air at room temperature (*A* is absorbance). See Table 2 for the assignment of absorption bands *1*–*8*.

Here, k denotes the rate constants of oxidation; K denotes the adsorption constants; C denotes gas-phase concentrations; the subscripts A and E refer to acetaldehyde and ethanol, respectively; and the superscripts denote the accessibility of reaction centers to adsorption. The first term reflects the contribution of oxidation at centers that are accessible to only ethanol or only acetaldehyde, and the second term reflects that at centers that are accessible to both of the molecules. All of the experimental curves in Fig. 10 are adequately described by Eqs. (1) with constant parameters. The exception is the rate W_E, which was chosen individually for each particular ethanol concentration. It is likely that the necessity of this choice was due to the fact that one of the products of ethanol oxidation (acetic acid) occupied a portion of the centers of ethanol adsorption. Therefore, the rate of ethanol oxidation at centers specific for ethanol decreased with increasing ethanol concentration.

For practical applications of the photocatalytic removal of ethanol vapor from air, it is of importance to choose oxidation conditions under which the minimum formation of an undesired intermediate product (acetaldehyde) and the maximum selectivity for the product of complete oxidation (CO_2) are observed. An increase in the intensity of catalyst irradiation with UV light increased the selectivity for CO_2; however, in this case, the overall quantum efficiency of ethanol oxidation decreased. In this case, the rate of photocatalytic oxidation of acetaldehyde increased more rapidly than the rate of ethanol oxidation because of an increase in the mole fraction of acetaldehyde in the steady-state composition of the gaseous reaction mixture.

Temperature is another easy-to-change parameter. Figure 11 demonstrates the effects of temperature on the steady-state rate of oxygen consumption and on the selectivity for oxidation to CO_2 in the photocatalytic oxidation of ethanol vapor on titanium dioxide. As in the case of acetone vapor, it can be seen that the rate of oxidation increased as the temperature was increased to 100°C and then decreased, probably, because of the thermal deactivation of the catalyst. The condensation of the resulting acetaldehyde on the catalyst surface is the most probable reason for TiO_2 deactivation [12]. The selectivity of oxidation with respect to CO_2 continuously decreased with temperature; this was likely due to the deactivation of reaction centers that were responsible for the deep oxidation of ethanol [12].

In the photocatalytic oxidation of ethanol on platinized TiO_2 (Fig. 12), the rate of oxidation was higher than that on pure TiO_2 by a factor of ~1.5. The selectivity of oxidation to CO_2 continuously increased with temperature, although the rate of oxidation somewhat decreased at a temperature higher than 80°C. In this case, the observed increase in the selectivity can be due to the thermal oxidation of acetaldehyde on platinum

particles. In the oxidation of ethanol on the above photocatalyst in the dark, the reaction rate and selectivity for CO_2 increased with temperature; however, both the rate of oxidation and the selectivity were lower than those on the irradiation of the catalyst with light by a factor of ~4.

It is most convenient to study the effect of titanium dioxide platinization on the product composition of photocatalytic ethanol oxidation by performing the reaction in a batch reactor. In addition to acetaldehyde, a small amount of CO was detected on pure titanium dioxide among the intermediate oxidation products released into the gas phase [11]. On the platinized catalyst, the rate of carbon dioxide release was two times higher and CO was not detected; however, acetic acid was detected in a low concentration in the gas phase. Thus, catalyst platinization not only accelerated photocatalytic oxidation but also eliminated the formation of CO, which is an undesirable product of the partial oxidation of the initial substrate.

Table 2. Assignment of absorption bands in the IR spectrum of the surface of TiO_2 in the photocatalytic oxidation of ethanol (Fig. 9)

Peak no.	ν, cm^{-1}	Structure responsible for absorption*
1	1753	Acetic acid
2	1725	Acetaldehyde
3	1660	$\diagdown$C=O- –Ti $\diagup$
4	1628	Water
5	1568	$RCOO^-$ (1) (antisymmetrical)
6	1517	$RCOO^-$ (2)
7	1437	CO_3^{2-}
8	1404	$RCOO^-$ (1) (symmetrical)

* Figures in parentheses refer to the types of adsorbed carboxylates.

4. Photocatalytic Mineralization of Organic Sulfides

The use of photocatalysis seems attractive for the degradation of chemical warfare agents because of the ability of heterogeneous photocatalysts to perform the complete oxidation (mineralization) of a wide variety of organic compounds. Because chemical warfare agents are extremely toxic substances, we used their low-toxicity analogues (simulants) in the experiments. The following three substances were used for simulating the chemical warfare agent yperite (mustard gas, bis(2-chloroethyl) sulfide): diethyl sulfide, 2-phenethyl

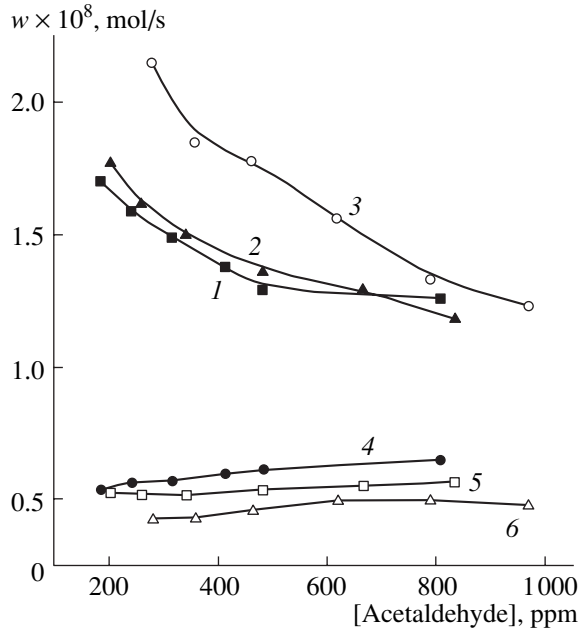

Fig. 10. Dependence of the rates of the first (w_1) and second steps (w_2) of oxidation of ethanol vapor in air on Hombifine N TiO_2 on acetaldehyde concentration at three concentrations of ethanol vapor: (*1*, *4*) 250, (*2*, *5*) 500, and (*3*, *6*) 1000 ppm ethanol (w_1 and w_2, respectively). Temperature, 40°C; water vapor concentration, 5000 ppm. Illumination was performed with filtered light from a DKSL-1000 xenon lamp (λ = 334 nm).

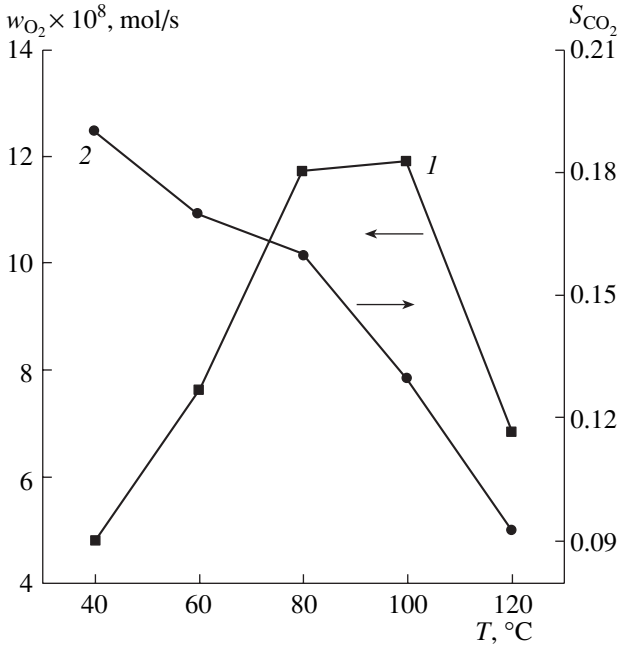

Fig. 11. Dependence of the steady-state rate of oxygen consumption (w_{O_2}) in the oxidation of ethanol in air and the selectivity of ethanol oxidation to CO_2 (S_{CO_2}) on the temperature of reaction on TiO_2. Ethanol concentration, 650 ppm; water vapor concentration, 4800 ppm. Illumination was performed with filtered light from a DKSL-1000 xenon lamp (λ = 334 nm).

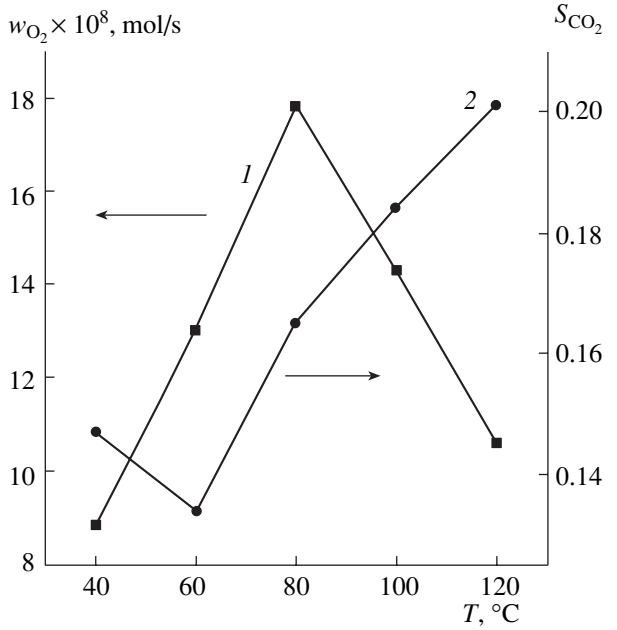

Fig. 12. Effect of temperature on the steady-state rate of oxygen consumption (w_{O_2}) in the oxidation of ethanol and the selectivity of ethanol oxidation to CO_2 (S_{CO_2}) on 1.1% Pt/TiO_2. Ethanol concentration, 740 ppm; water vapor concentration, 4900 ppm. Illumination was performed with filtered light from a DKSL-1000 xenon lamp (λ = 334 nm).

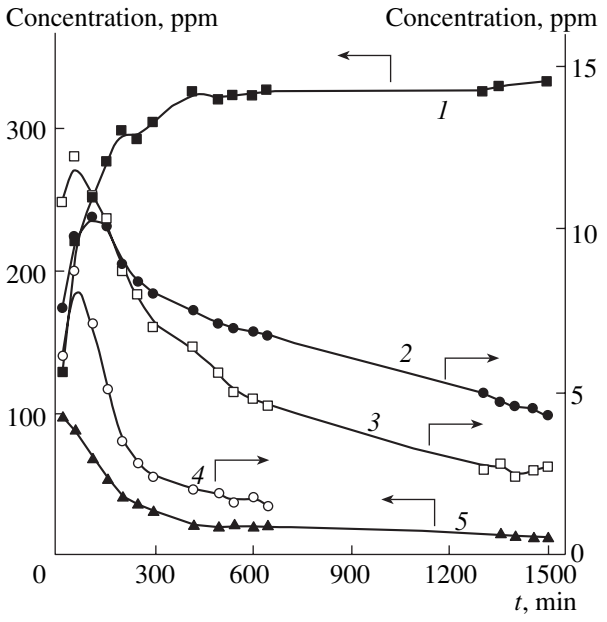

Fig. 13. Concentrations of diethyl sulfide vapor and its decomposition products at the outlet of a photocatalytic flow reactor: (*1*) diethyl sulfide, (*2*) ethylene, (*3*) diethyl disulfide, (*4*) ethanol, and (*5*) acetaldehyde. Reactor temperature, 25°C; air humidity, 59%; photocatalyst, Hombikat UV 100 TiO_2.

2-chloroethyl sulfide, and 2-chloroethyl ethyl sulfide. The photocatalytic mineralization of their vapors in air was performed in batch and flow reactors.

In the photocatalytic oxidation of diethyl sulfide vapor in a flow reactor (Fig. 13) with a short contact time, diethyl sulfide and a few gaseous photocatalytic oxidation intermediates (ethylene, ethanol, and acetaldehyde) were detected at the reactor outlet. The final oxidation product (CO_2) was detected in small amounts only at the very beginning of the reaction. The oxidation of diethyl sulfide did not take place without irradiation of the photocatalyst. As can be seen in Fig. 13, the concentration of diethyl sulfide in the gas phase at the reactor outlet gradually increased in the course of the reaction and the concentration of oxidation products decreased; that is, catalyst deactivation was observed.

To find a catalyst that is most stable to deactivation, we tested Degussa P25 titanium dioxides (50 and 75 m^2/g), Hombikat UV 100 titanium dioxide (347 m^2/g), and homemade TiO_2 (120 m^2/g) under identical conditions. The photocatalysts were compared with respect to the amounts of diethyl sulfide converted in the reaction in 455 min. We found that the amount of converted diethyl sulfide was proportional to the total surface area of the photocatalyst; in this case, Hombikat UV 100 TiO_2 was deactivated at the lowest rate [13]. This was due to the fact that the photocatalyst with a large surface area (347 m^2/g) can bind a greater amount of deactivating products in adsorbed states. Therefore, the experiments with sulfides described below were performed with the use of Hombikat UV 100 TiO_2.

High air humidity had an adverse effect on the conversion of diethyl sulfide; an optimum humidity was found to be about 20%. An increase in the intensity of light by a factor of 10 resulted in an increase in diethyl sulfide conversion by a factor of only ~1.5.

The photocatalytic oxidation of diethyl sulfide was also studied in a batch reactor and *in situ* in a cell of an IR spectrometer [14]. Diethyl sulfide was completely photooxidized to inorganic products at a sufficient duration of the experiment. Ethylene and acetaldehyde were detected as gaseous intermediate products of the photocatalytic oxidation.

Deactivation in a batch reactor was studied by the successive complete oxidation of several equal portions of the parent substance on the same photocatalyst. Figure 14 shows the kinetic curves of diethyl sulfide consumption and CO_2 buildup. It can be seen that, from cycle to cycle, the rate of consumption of the parent substance and the average rate of CO_2 release decreased. It is of interest that all of the curves that illustrate CO_2 concentration changes exhibit two portions and the rates of CO_2 release at these portions are similar in all of the curves. It is believed that the rate of CO_2 release at the initial portion was low because of the consumption of photogenerated primary charge carriers mainly for the primary partial oxidation of diethyl

sulfide molecules. The rate of CO_2 release increased only after completion of this primary oxidation of diethyl sulfide. Indeed, among all of the organic substances present on the surface of TiO_2 in the course of photocatalytic oxidation, diethyl sulfide molecules exhibit the lowest ionization potential [14]. Therefore, intermediate products were oxidized more slowly than the parent substrate. The quantum efficiency of the photocatalytic oxidation of diethyl sulfide decreased from 3.3% in the first cycle to 0.27% in the fifth cycle. The total weight of diethyl sulfide mineralized in the five cycles of photocatalytic oxidation was a third of the weight of titanium dioxide. Assuming that the concentration of active centers on the photocatalyst surface is equal to 5×10^{14} cm^{-2} [15], we can evaluate the ratio of the number of moles of oxidized diethyl sulfide to the amount of active centers of the TiO_2 sample. This ratio was equal to 1. In other words, the turnover number of each active center before its deactivation was equal to unity.

The most likely reason for the deactivation of TiO_2 is the accumulation of the complete oxidation products of diethyl sulfide on the surface. Figure 15 demonstrates the diffuse-reflectance IR spectra of the surface of titanium dioxide upon completion of each cycle of the photocatalytic oxidation of diethyl sulfide. It can be seen that three intense absorption bands at 1045, 1135, and 1226 cm^{-1} were observed. The first two absorption bands are usually attributed to adsorbed monodentate sulfates [16], whereas the band at 1226 cm^{-1} can be ascribed to adsorbed sulfonic acid [17]. Indeed, this absorption band was not observed after completion of the first cycle, in which carbon was almost completely converted into CO_2; however, it was observed in the subsequent cycles, in which the oxidation of adsorbed organic substances occurred incompletely.

The oxidation of diethyl sulfide in a coil reactor allowed us to identify a greater number of both volatile and strongly sorbed intermediates and final products of diethyl sulfide oxidation [18]. Before the complete deactivation of the photocatalyst, only CO_2 (the gaseous product of complete oxidation) was detected at the reactor outlet in accordance with the stoichiometry of deep oxidation:

$$C_4H_{10}S + 8O_2 \longrightarrow 4CO_2 + 4H_2O + H_2SO_4.$$

After photocatalyst deactivation, the concentration of CO_2 at the reactor outlet dramatically decreased and many gaseous products of partial oxidation were detected. Among them, the main products were acetaldehyde, diethyl disulfide, SO_2, ethylene, and acetic acid. The following nonvolatile and low-volatility products were detected in wash water from the surface: diethyl disulfide, diethyl trisulfide, diethyl sulfoxide, ethanesulfonic acid, ethanesulfinic acid, diethylsulfone, etc.

The washing of the deactivated photocatalyst with water almost completely restored its activity. However, after more than ten photocatalyst deactivation–reactivation cycles were performed, the time of catalyst operation in diethyl sulfide oxidation until deactivation somewhat shortened, likely, because of the etching of the photocatalyst surface by sulfuric acid formed in the reaction. It was also found that a decrease in the concentration of diethyl sulfide in the starting reaction mixture resulted in that a greater amount of diethyl sulfide

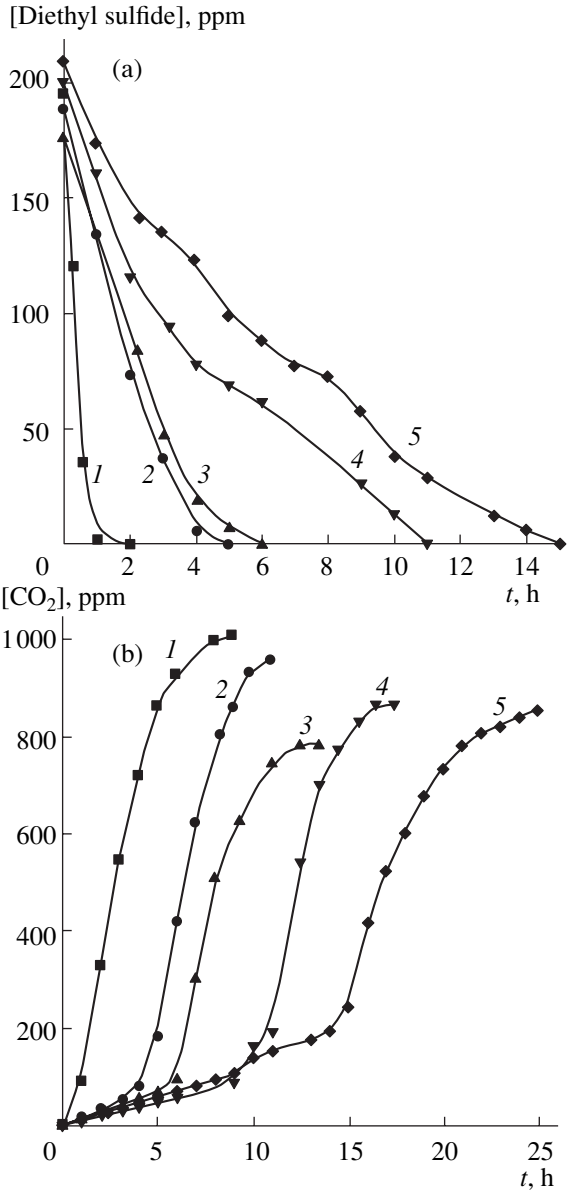

Fig. 14. Changes in the concentrations of (a) diethyl sulfide vapor and (b) CO_2 in air in the course of the photocatalytic oxidation of five 0.5-μl portions of diethyl sulfide successively injected into air in a batch reactor. Curve numbers correspond to the portion numbers of diethyl sulfide oxidized. Illumination was performed with filtered light from a DKsEl-1000 xenon lamp; the light intensity was 70 mW/cm^2 ($\lambda < 400$ nm). Catalyst weight, 7.5 mg; illuminated photocatalyst surface area, 7.5 cm^2; temperature, 35°C.

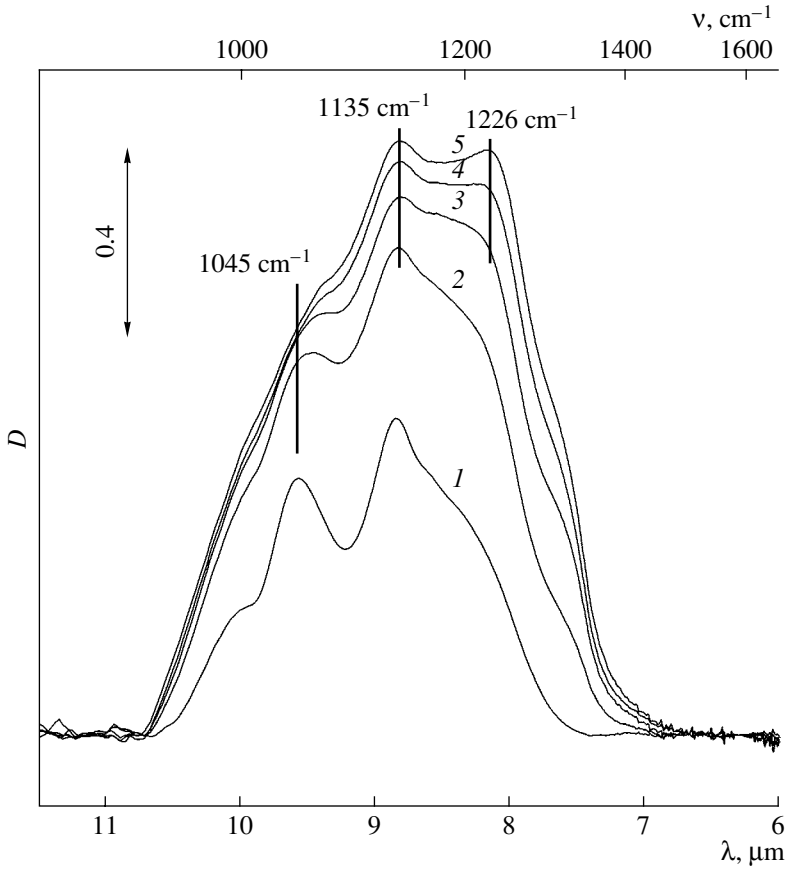

Fig. 15. Diffuse-reflectance IR spectra of Hombikat UV 100 TiO_2 after the photocatalytic oxidation of each of the five portions of diethyl sulfide in a batch reactor (Fig. 14). The spectrum of the initial TiO_2 sample was subtracted from all of the IR spectra.

underwent mineralization before photocatalyst deactivation. An increase in the weight of the photocatalyst in the reactor also significantly increased the time before deactivation in diethyl sulfide oxidation. It is believed that an increase in the weight of the photocatalyst caused an increase in the illuminated surface area of the photocatalyst and, consequently, increased the conversion of diethyl sulfide because of more efficient utilization of light from the lamp. However, individual experiments on the photocatalytic oxidation of acetone demonstrated that the rate of acetone oxidation after increasing the weight of the photocatalyst supported on the walls practically did not increase. Consequently, it may be expected that, in the case of diethyl sulfide, an increase in the rate of oxidation also occurred because of an important role of the stage of the transfer of complete and partial oxidation products to unilluminated portions of the photocatalyst rather than because of an increase in the illuminated surface area of the catalyst. It is believed that partial oxidation products were transferred to unilluminated portions of the photocatalyst to free the illuminated surface of the catalyst for photocatalytic oxidation.

The nature of the detected products of the photocatalytic degradation of diethyl sulfide allowed us to propose a conceivable scheme of the photocatalytic process (Scheme 1). The process begins with the removal of an electron from the sulfur atom by a mobile hole. The resulting radical cation is further transformed by the cleavage of the C–S bond and/or oxygen addition at the sulfur atom (i.e., sulfur oxidation). Reactions with an increase in the oxidation state of carbon atoms can occur simultaneously. The final oxidation products are SO_2, water, carbon dioxide, and sulfuric acid.

In general, the TiO_2 photocatalytic oxidation of 2-phenethyl-2-chloroethyl sulfide occurred via the same reaction paths as the photocatalytic oxidation of diethyl sulfide vapor. In the photooxidation in a flow reactor, chloroethylene, acetic acid, 2-chloroethanol, benzaldehyde, benzoic acid, and styrene were detected as products. High air humidity and a decrease in the reaction temperature were favorable for the inhibition of photocatalyst deactivation [19]. Under these conditions, water can compete for adsorption sites on the surface of the photocatalyst and keep a portion of the surface free from a strongly adsorbed substrate. Oxygen molecules, which are required for oxidation, can be adsorbed simultaneously at sites occupied by water. It is believed that some oxidation products are dissolved in a water film on the surface of TiO_2; thereby, active

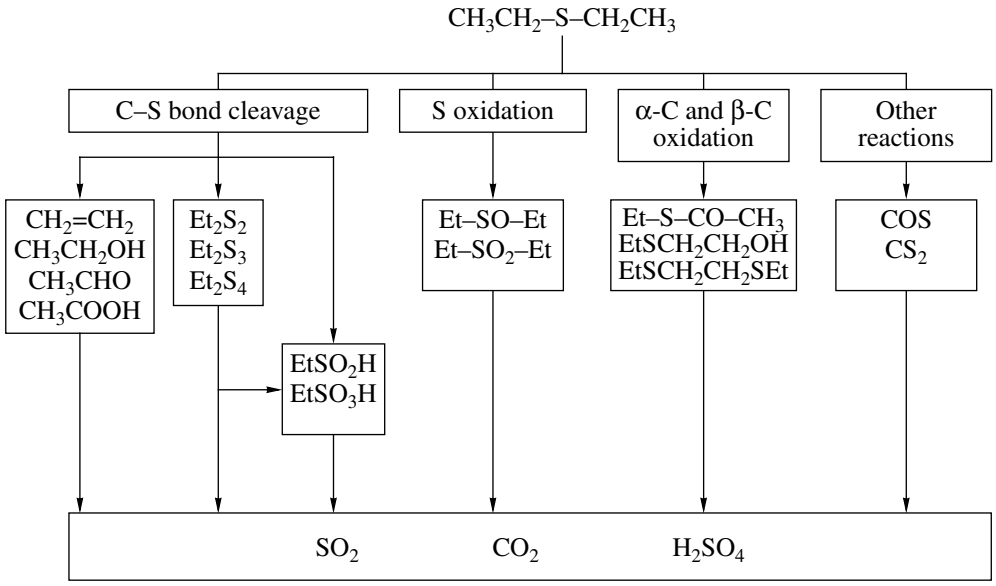

Scheme 1. Schematic diagram of the main reaction paths and the products of the TiO_2 photocatalytic degradation of diethyl sulfide vapor in air.

centers become free for the occurrence of oxidation reactions.

Many volatile and nonvolatile oxidation intermediates were detected in the photocatalytic oxidation of 2-chloroethyl ethyl sulfide vapor in a coil reactor [20]. The main products that desorbed into the gas phase were CO_2, SO_2, chloroethylene, acetaldehyde, chloroacetaldehyde, acetic acid, diethyl disulfide, and 2-chloroethyl ethyl disulfide. Unlike the photocatalytic oxidation of diethyl sulfide, considerable amounts of the unoxidized parent substrate were extracted from the surface of TiO_2 after completion of a 2-chloroethyl sulfide oxidation cycle. Moreover, 2-chloroethyl ethyl sulfoxide and bis(2-chloroethyl) disulfide were also sorbed in considerable amounts. Evidently, the presence of the parent substrate on the surface of the photocatalyst after a photocatalytic oxidation cycle is performed is due to the lower reactivity of substrate molecules toward oxidation (as compared to the reactivity of partial oxidation products) because of an electron density shift to the chlorine atom. It was found that 2-chloroethyl ethyl sulfide was partially hydrolyzed (by 17%) on the surface of TiO_2 when the reaction was performed in the dark at room temperature. As in the case of diethyl sulfide, a decrease in the concentration of 2-chloroethyl sulfide in the starting reaction mixture makes it possible to mineralize a greater amount of the parent substrate before photocatalyst deactivation.

The IR spectroscopy of the photocatalyst surface in the course of reaction revealed the accumulation of various sorbed partial oxidation products and sulfuric acid. The "annealing" of the deactivated photocatalyst under UV light in air without substrate supply resulted in a decrease in the intensities of bands that correspond to organic compounds and in an increase in the absorption band of monodentate sulfates. The washing of the catalyst with water after completion of the oxidation of products adsorbed on the surface resulted in the removal of monodentate sulfates, and the remaining low-intensity absorption bands corresponded to bidentate sulfates. Thus, sorbed bidentate sulfates can contribute to the development of photocatalyst deactivation, which cannot be removed by washing with water.

The nature of the detected products of photocatalytic oxidation allowed us to propose a few main reaction paths for the conversion of 2-chloroethyl ethyl sulfide on the surface of illuminated titanium dioxide: the hydrolysis of the carbon–sulfur bond, the cleavage of the sulfur–carbon bond, the oxidation of sulfur atoms, and the oxidation of carbon atoms (Scheme 2). This reaction scheme also corresponds to the photocatalytic oxidation of 2-phenethyl-2-chloroethyl sulfide vapor in air.

5. Photocatalytic Degradation of Dimethyl Methylphosphonate Vapor

Many chemical warfare agents are organophosphorus compounds containing a pentavalent phosphorus atom bound to alkyl and alkoxy groups. These are, for example, sarin, soman, tabun, and VX. Dimethyl methylphosphonate, which contains a methyl group and methoxy groups, can simulate some properties of these chemical warfare agents.

We studied the photocatalytic degradation of dimethyl methylphosphonate vapor in air in a small batch reactor containing 7.4 g of Hombikat UV 100 TiO_2. After 0.5 μl of dimethyl methylphosphonate was evap-

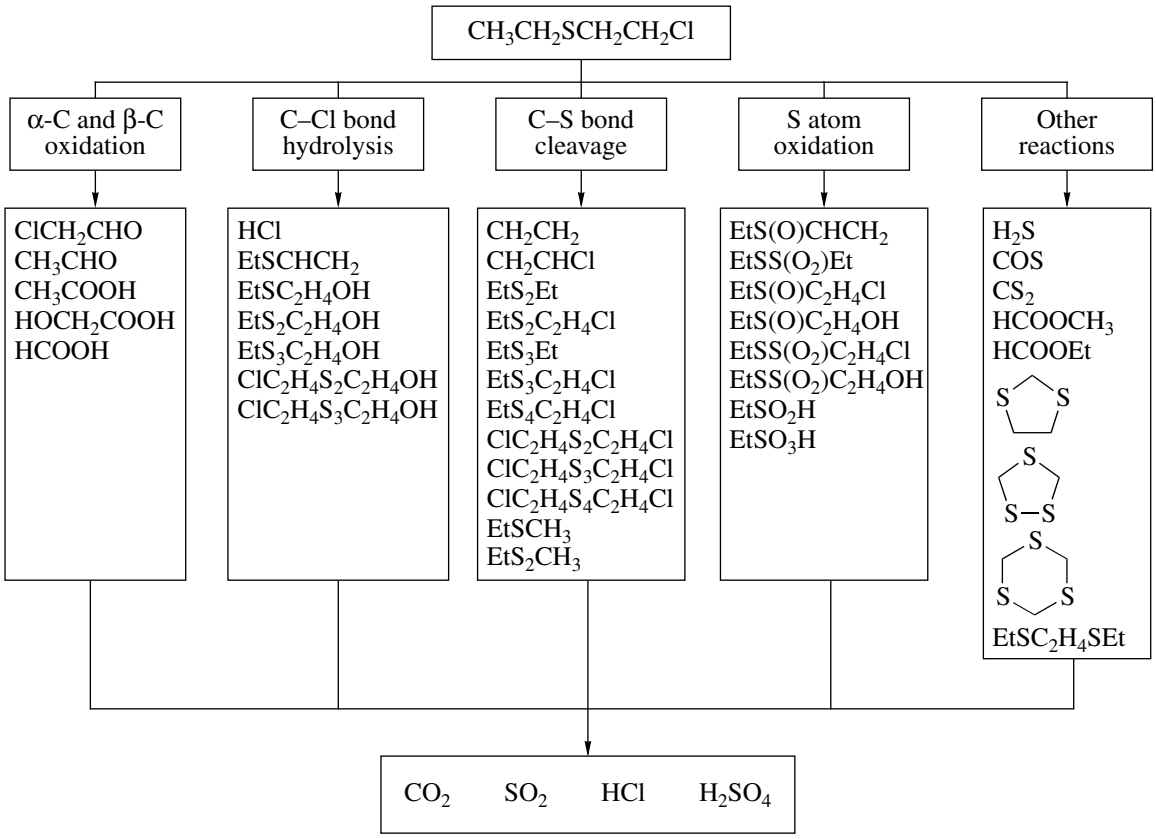

Scheme 2. Schematic diagram of the main reaction paths and the products of the TiO_2 photocatalytic degradation of chloroethyl ethyl sulfide vapor in air.

orated in the reactor at room temperature, the substrate was completely adsorbed on the surface of TiO_2 and absent from the gas phase. Figure 16 shows the kinetic curves of CO_2 buildup in the gas phase after the onset of UV irradiation of the photocatalyst in the successive oxidation of four 0.5-μl portions of dimethyl methylphosphonate on the same photocatalyst sample. It can be seen that the CO_2 buildup curves corresponding to the oxidation of the first two portions of dimethyl methylphosphonate are practically coincident. The oxidation of the subsequent portions was accompanied by the inhibition of carbon dioxide release. This was likely due to photocatalyst deactivation because of the accumulation of phosphoric acid (the product of the complete oxidation of dimethyl methylphosphonate) on the surface of the photocatalyst. It can also be seen that, even after partial deactivation of the photocatalyst, the photocatalytic mineralization of dimethyl methylphosphonate occurred much more rapidly than the photocatalytic oxidation of diethyl sulfide under similar conditions (cf. Fig. 14).

We found that methanol was released into the gas phase even before the onset of photocatalyst irradiation. This fact is indicative of the intense dark hydrolysis of dimethyl methylphosphonate. Figure 17 shows the kinetic curves of dark hydrolysis in air with 30% relative humidity in the presence and in the absence of titanium dioxide. It can be seen that the concentration of methanol vapor released upon the hydrolysis on titanium dioxide was higher than the concentration of methanol vapor formed with no catalyst by three orders of magnitude. Because the catalyst cannot shift the equilibrium of hydrolysis in the gas phase, it is believed that the strong adsorption of a hydrolysis product occurred on the surface of the photocatalyst to shift the observed position of the hydrolysis "equilibrium."

To test the above hypothesis, using statistical thermodynamics methods and assuming that all of the substances occurred in the gas phase, we calculated the equilibrium constants of the two-step dissociation of dimethyl methylphosphonate:

$$(CH_3O)_2P(O)CH_3 + H_2O$$
$$= CH_3OP(O)(OH)CH_3 + CH_3OH,$$
$$CH_3OP(O)(OH)CH_3 + H_2O$$
$$= (HO)_2P(O)CH_3 + CH_3OH.$$

The equilibrium constants of the first and second steps were found to be $K_{eq}^{(1)} = 8.9 \times 10^{-8}$ and $K_{eq}^{(2)} = 6.1 \times 10^{-7}$, respectively. The equilibrium gas-phase concentration of methanol vapor calculated using the above constants,

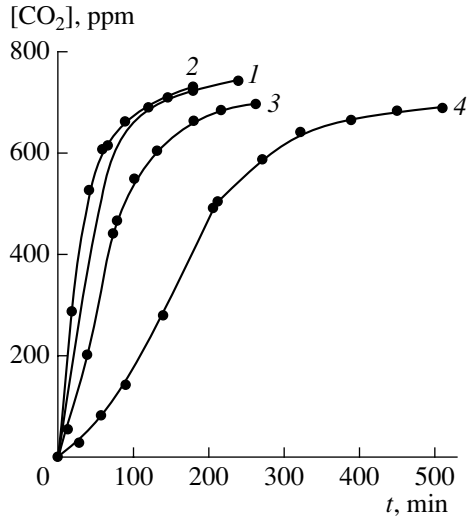

Fig. 16. Kinetic curves of the buildup of carbon dioxide in the course of the photocatalytic oxidation of four 0.5-μl portions of liquid dimethyl methylphosphonate successively injected into air in a 434-cm^3 batch reactor. Curve numbers correspond to the portion numbers of the substrate oxidized. The illumination conditions and temperature are specified in Fig. 14.

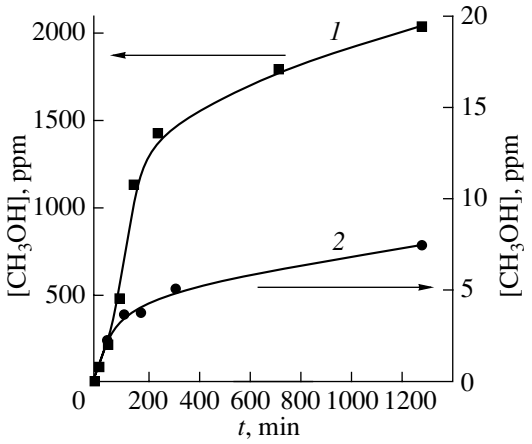

Fig. 17. Accumulation of methanol vapor in a 164-ml batch reactor in the course of the dark hydrolysis of dimethyl methylphosphonate in air: (*1*) in the presence of 200 mg of Hombikat UV 100 TiO_2 and (*2*) in the empty reactor without TiO_2. Relative air humidity in the reactor, 30%; room temperature.

which corresponds to the conditions specified in Fig. 17, was 4 ppm. This value is consistent with the experimental value of 7 ppm.

Acid and/or basic sites on the surface catalyze hydrolysis. We studied the effect of the surface acidity of titanium dioxide on the rate of hydrolysis of dimethyl methylphosphonate at room temperature. The amounts of acid and basic sites on the surface of titanium dioxide were controlled by treatment with sulfuric acid or sodium hydroxide.

Table 3. Initial rate (w_0) of the dark hydrolysis of dimethyl methylphosphonate vapor on TiO_2 samples treated with aqueous solutions of sulfuric acid and sodium hydroxide at various air humidities and room temperature

Solution composition for the treatment of TiO_2	$w_0 \times 10^9$, mol l^{-1} min^{-1}	
	Air humidity, %	
	0	50
10 M H_2SO_4	3.02	2.06
1 M H_2SO_4	21.1	3.84
Untreated	166	48.2
1 M NaOH	210	65.5
4 M NaOH	171	41.0
10 M NaOH	53.8	37.4

Note: In the course of testing, 2 μl of dimethyl methylphosphonate was introduced into a 434-ml batch reactor with a 7.5-mg TiO_2 sample arranged within the reactor and the rate of buildup of methanol vapor was measured. Humidity was regulated by purging the reactor with air with a corresponding concentration of water vapor.

Table 3 summarizes the results of testing titanium dioxide in the hydrolysis reaction. Although water is a necessary reactant in the hydrolysis reaction, an increase in the relative humidity of air to 50% significantly decreased the rate of this reaction. This can be due to the water poisoning of surface centers that are responsible for hydrolysis. Indeed, an attempt to perform the hydrolysis of dimethyl methylphosphonate in an aqueous suspension of titanium dioxide did not result in a detectable change in the substrate concentration even after 23 days [21]. The treatment of the surface of TiO_2 with sulfuric acid also dramatically inhibited the hydrolysis. In contrast, the treatment of TiO_2 with a moderate amount of an alkali ($[OH^-]$ = 1 mol/l) increased the rate of hydrolysis. However, at a sodium hydroxide concentration higher than 4 mol/l, the rate of hydrolysis became lower than that on untreated titanium dioxide. It is believed that a moderate amount of acid sites on the surface of TiO_2 is a necessary condition for the rapid dark hydrolysis of the test substrate. The activity of titanium dioxide in the photocatalytic oxidation of acetone vapor changed oppositely to changes in the rate of hydrolysis and reached a maximum in a sample treated with 10 M sulfuric acid.

CONCLUSIONS

We studied the TiO_2 photocatalytic oxidation of gaseous model substrates in a flow of air. We found the following:

The rate of the TiO_2 photocatalytic oxidation of CO increased as the concentration of CO was increased from 0 to 0.4 vol % in accordance with the Langmuir–Hinshelwood model with a single type of reaction cen-

ters and monotonically increased with reaction temperature. The platinization of TiO_2 considerably increased the photocatalytic activity in the oxidation of CO.

The rate of oxidation of acetone vapor under steady-state conditions was adequately described by the Langmuir–Hinshelwood model with two types of reaction centers on the surface of TiO_2. The deactivation of TiO_2 began at temperatures higher than 100°C; the rate of deactivation decreased as the concentration of acetone vapor was decreased or the concentration of water vapor in the gas phase was increased. On platinized TiO_2, deactivation may not occur because of a high rate of dark reactions at elevated temperatures.

The TiO_2 photocatalytic oxidation of ethanol was adequately described by the semiempirical Langmuir–Hinshelwood model that takes into consideration the occurrence of three types of active centers: centers accessible to both ethanol and acetaldehyde and centers accessible to only ethanol or only acetaldehyde. An increase in the intensity of UV irradiation of TiO_2 increased selectivity for the deep photocatalytic oxidation of ethanol to CO_2.

Organic sulfide vapors underwent complete photocatalytic mineralization on TiO_2 and gradually deactivated the catalyst, whose activity can be restored by washing with water. The photocatalytic oxidation of these sulfides began with the oxidation of the sulfur atom by photogenerated holes. Among the TiO_2 samples tested, Hombikat UV 100 TiO_2 exhibited a maximum activity in the photocatalytic oxidation of sulfides because it possessed the highest specific surface area.

The photocatalytic degradation of dimethyl methylphosphonate vapor was accompanied by dark hydrolysis with the formation of methanol. The highest activity in hydrolysis or photooxidation was found in TiO_2 pretreated with an alkali or an acid, respectively.

ACKNOWLEDGMENTS

This work was supported by the Russian Foundation for Basic Research (project no. 02-03-08002), the program "Leading Scientific Schools of Russia" (grant no. NSh 1484.2003.3), and the Academy of Finland (grant no. 208134). A.V. Vorontsov acknowledges the support of the Foundation for the Support of Domestic Science. D.V. Kozlov acknowledges the support of the CRDF (grant no. NO-008-X1).

REFERENCES

1. Miller, R. and Fox, R., *Photocatalytic Purification and Treatment of Water and Air*, Ollis, D.F. and Al-Ekabi, H., Eds., Amsterdam: Elsevier, 1993, p. 573.
2. Vorontsov, A.V., Savinov, E.N., Kurkin, E.N., Horbova, O.D., and Parmon, V.N., *React. Kinet. Catal. Lett.*, 1997, vol. 62, no. 1, p. 83.
3. Vorontsov, A.V., Savinov, E.N., Barannik, G.B., Troitsky, V.N., and Parmon, V.N., *Catal. Today*, 1997, vol. 39, p. 207.
4. Vorontsov, A.V. and Savinov, E.N., *Chem. Eng. J.*, 1998, vol. 70, no. 3, p. 231.
5. Vorontsov, A.V., Kozlov, D.V., Smirniotis, P.G., and Parmon, V.N., *Kinet. Catal.*, 2005, vol. 46, no. 2, p. 203.
6. Vorontsov, A.V., Kurkin, E.N., and Savinov, E.N., *J. Catal.*, 1999, vol. 186, p. 318.
7. Vorontsov, A.V., Stoyanova, I.V., Kozlov, D.V., Simagina, V.I., and Savinov, E.N., *J. Catal.*, 2000, vol. 189, p. 360.
8. Kozlov, D.V., Paukshtis, E.A., and Savinov, E.N., *Appl. Catal., B*, 2000, vol. 24, p. 7.
9. Nimlos, M.R., Wolfrum, E.J., Brewer, M.L., Fennell, J.A., and Bintner, G., *Environ. Sci. Technol.*, 1996, vol. 30, p. 3102.
10. Peral, J. and Ollis, D.F., *J. Catal.*, 1992, vol. 136, p. 554.
11. Vorontsov, A.V. and Dubovitskaya, V.P., *J. Catal.*, 2004, vol. 221, no. 1, p. 102.
12. Muggli, D.S. and Falconer, J.L., *J. Catal.*, 1998, vol. 175, p. 213.
13. Vorontsov, A.V., Savinov, E.N., Davydov, L., and Smirniotis, P.G., *Appl. Catal., B*, 2001, vol. 32, p. 11.
14. Kozlov, D.V., Vorontsov, A.V., Smirniotis, P.G., and Savinov, E.N., *Appl. Catal., B*, 2003, vol. 42, p. 77.
15. Sauer, M.L. and Ollis, D.F., *J. Catal.*, 1996, vol. 163, p. 215.
16. Nakamoto, K., *Infrared and Raman Spectra of Inorganic and Coordinated Compounds*, New York: Wiley, 1986.
17. Socrates, G., *Infrared Characteristic Group Frequencies*, New York: Wiley, 1994.
18. Vorontsov, A.V., Savinov, E.N., Lion, C., and Smirniotis, P.G., *Appl. Catal., B*, 2003, vol. 44, p. 25.
19. Vorontsov, A.V., Panchenko, A.A., Savinov, E.N., Lion, C., and Smirniotis, P.G., *Environ. Sci. Technol.*, 2002, vol. 36, no. 23, p. 5261.
20. Vorontsov, A.V., Lion, C., Savinov, E.N., and Smirniotis, P.G., *J. Catal.*, 2003, vol. 44, no. 1, p. 25.
21. Vorontsov, A.V., Davydov, L., Reddy, E.P., Lion, C., Savinov, E.N., and Smirniotis, P.G., *New J. Chem.*, 2002, vol. 26, no. 6, p. 732.